Front. Mech. Eng. 2021, 16(1): 186–195
https://doi.org/10.1007/s11465-020-0608-0

RESEARCH ARTICLE

Yuhan JIA, Peng ZHAO, Jun XIE, Xuechun ZHANG, Hongwei ZHOU, Jianzhong FU

Single-electromagnet levitation for density measurement and defect detection

Abstract This paper presents a single-electromagnet levitation device to measure the densities and detect the internal defects of antimagnetic materials. The experimental device has an electromagnet in its lower part and a pure iron core in the upper part. When the electromagnet is activated, samples can be levitated stably in a paramagnetic solution. Compared with traditional magnetic levitation devices, the single-electromagnet levitation device is adjustable. Different currents, electromagnet shapes, and distances between the electromagnet and iron core are used in the experiment depending on the type of samples. The magnetic field formed by the electromagnet is strong. When the concentration of the $MnCl_2$ aqueous solution is 3 mol/L, the measuring range of the single-electromagnet levitation device ranges from 1.301 to 2.308 g/cm^3. However, with the same concentration of $MnCl_2$ aqueous solution (3 mol/L), the measuring range of a magnetic levitation device built with permanent magnets is only from 1.15 to 1.50 g/cm^3. The single-electromagnet levitation device has a large measuring range and can realize accurate density measurement and defect detection of high-density materials, such as glass and aluminum alloy.

Keywords single-electromagnet, electromagnetic levitation, density measurement, defect detection

Received May 18, 2020; accepted August 17, 2020

Yuhan JIA, Peng ZHAO (✉), Jun XIE, Xuechun ZHANG, Hongwei ZHOU, Jianzhong FU
The State Key Laboratory of Fluid Power and Mechatronic Systems, Zhejiang University, Hangzhou 310027, China; Key Laboratory of 3D Printing Process and Equipment of Zhejiang Province, Zhejiang University, Hangzhou 310027, China
E-mail: pengzhao@zju.edu.cn

Peng ZHAO
Jiangsu Jianghuai Magnetic Industry Co., Ltd., Huaian 211700, China

Hongwei ZHOU
Tederic Machinery Co., Ltd., Hangzhou 311224, China

1 Introduction

Magnetic levitation is a promising method for density measurement [1] and defect detection [2]. Compared with other measurement methods, such as density gradient and immersion and weighing, magnetic levitation is faster, more sensitive, and easier to operate [3]. A diamagnetic material can be levitated stably in a paramagnetic solution because of the effect of a magnetic field [4,5]. The sample is not damaged during density measurement and defect detection.

Traditional magnetic levitation devices are composed of two permanent NdFeB magnets positioned with like poles facing each other [6]. Transverse magnetic levitation devices (which measure density by horizontal displacement) [7] and axial magnetic levitation devices [8,9] are available at present. A paramagnetic solution is placed between two permanent magnets. When the distance between the two magnets is 45 mm, the magnetic field is linear [10]. When the distance between the two magnets is 60 mm, the magnetic levitation device has high sensitivity [11,12]. The magnetic levitation method can be used in the detection of forensic evidence [13], separation of a polycrystalline mixture [14,15], 3D orientation of objects [16,17], non-destructive testing [18], density measurement [19,20] with smartphones [21], and separation of polymer waste [22]. Traditional magnetic levitation devices have several limitations. Permanent magnets cannot generate large magnetic fields. The magnetic induction intensity of the magnet surface is only 0.4 T [1]. Samples with high density (more than 2 g/cm^3) cannot be levitated stably. Moreover, transverse magnetic levitation devices cannot form a large magnetic field [23]. The formation of a large magnetic field could expand the measuring range of magnetic levitation technology.

Compared with permanent magnets, electromagnets can adjust the magnetic field more conveniently and have stronger magnetic induction. This study describes the structure of a single-electromagnet levitation device and the distribution of magnetic induction intensity. The device

can form a large magnetic field and has good adjustability. Levitation of high-density materials is realized by changing the current and the distance between the electromagnet and iron core. Non-destructive defect detection and density measurement of samples are conducted experimentally by using the single-electromagnet levitation device.

2 Experimental methods

2.1 Single-electromagnet levitation device

A diagram of the device is shown in Fig. 1. Only one electromagnet is used in the electromagnet levitation device. The electromagnet pole is placed in the lower part of the experimental device, and a pure iron core is placed in the upper part. The shape and size of the two parts are the same, and they are both conical with a bottom radius of 65 mm and a height of 40 mm. The distance between upper and lower iron cores can be adjusted from 20 to 100 mm. The direction of the center line of the experimental device is aligned with the gravitational field. A container with a paramagnetic medium is placed on the electromagnet below. A base created via 3D printing is used in the experiment to enable the container to be placed stably. A $MnCl_2$ aqueous solution with different concentrations is used as the medium in this experiment. A programmable power supply is also utilized for current adjustment between 0 and 15 A. The device contains a water-cooled device, which guarantees the normal working temperature of the electromagnet. A magnetometer is used to measure the magnetic induction intensity in the middle of the single-electromagnet device. A digital camera is utilized for image recording.

2.2 Theory and methodology

Several samples can be levitated stably in a magnetic field. These materials are usually diamagnetic or weakly magnetic and require the assistance of a paramagnetic medium. When the levitation of a sample is stable, the gravity of the sample and the buoyancy and antimagnetic force are balanced. The forces are expressed as

$$\boldsymbol{F}_{\mathrm{mag}} = \frac{\chi_{\mathrm{s}} - \chi_{\mathrm{m}}}{\mu_0} V(\boldsymbol{B}\cdot\nabla)\boldsymbol{B}, \tag{1}$$

$$\boldsymbol{F}_{\mathrm{f}} = -\rho_{\mathrm{m}} V\boldsymbol{g}, \tag{2}$$

$$\boldsymbol{F}_{\mathrm{g}} = \rho_{\mathrm{s}} V\boldsymbol{g}, \tag{3}$$

where $\boldsymbol{F}_{\mathrm{mag}}$ is antimagnetic force, $\boldsymbol{F}_{\mathrm{f}}$ is floatage, $\boldsymbol{F}_{\mathrm{g}}$ is gravity, ρ_{m} represents the density of the paramagnetic medium, ρ_{s} represents the density of the sample, χ_{m} denotes the susceptibility of the paramagnetic medium, χ_{s} denotes the susceptibility of the sample, $\boldsymbol{B}$ is the magnetic induction intensity, B_x, B_y, and B_z represent the magnetic induction intensity in X, Y, and Z directions, $\boldsymbol{g}$ (9.8 m/s^2) represents the acceleration due to gravity, V represents the volume of the sample, and μ_0 ($4\pi\times10^{-7}$ N/A^2) is the permeability of a vacuum. $(\boldsymbol{B}\cdot\nabla)\boldsymbol{B}$ in Eq. (1) can be calculated using

$$(\boldsymbol{B}\cdot\nabla)\boldsymbol{B} = \begin{pmatrix} B_x\frac{\partial B_x}{\partial x} & B_y\frac{\partial B_x}{\partial y} & B_z\frac{\partial B_x}{\partial z} \\ B_x\frac{\partial B_y}{\partial x} & B_y\frac{\partial B_y}{\partial y} & B_z\frac{\partial B_y}{\partial z} \\ B_x\frac{\partial B_z}{\partial x} & B_y\frac{\partial B_z}{\partial y} & B_z\frac{\partial B_z}{\partial z} \end{pmatrix}. \tag{4}$$

In the magnetic field formed by an electromagnet, B_x and B_y on the centerline are not zero. The transverse movement of the sample is limited by the vessel wall during the experiment. The antimagnetic force on the sample in X and Y directions is in equilibrium with the supporting force on the vessel wall. Friction is reduced in the vertical direction by shaking and stirring. Therefore, in the process of density measurement and defect detection,

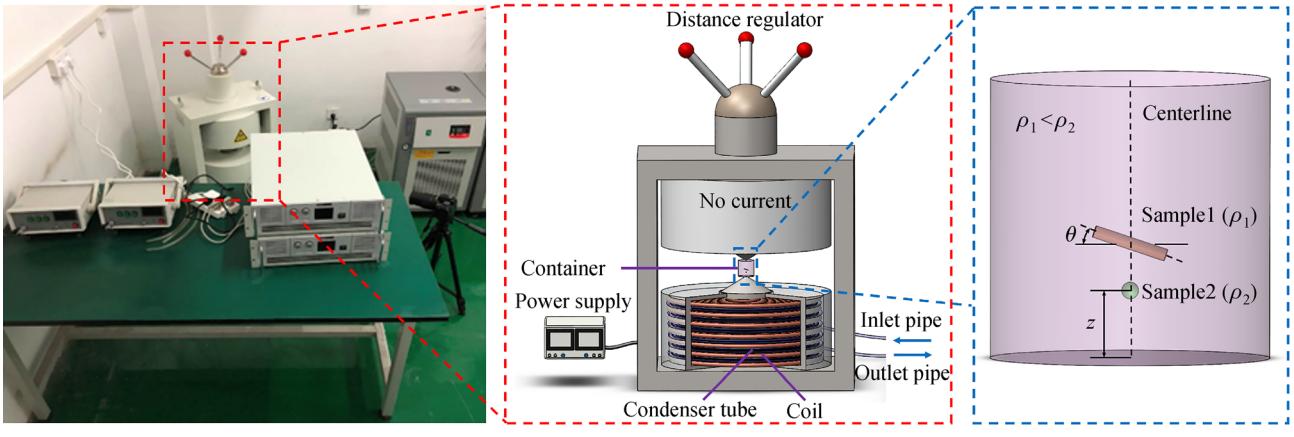

Fig. 1 Single-electromagnet levitation device.

the levitation height of the sample is only related to density. The levitation equilibrium position of the sample is at the edge of the container. The forces on the sample are expressed as follows:

$$F_{\mathrm{mag}} = \frac{\chi_{\mathrm{s}} - \chi_{\mathrm{m}}}{\mu_0} V \left(B_z \frac{\partial B_z}{\partial z} + B_x \frac{\partial B_z}{\partial x} + B_y \frac{\partial B_z}{\partial y} \right), \quad (5)$$

$$\boldsymbol{F}_{\mathrm{mag}} + \boldsymbol{F}_{\mathrm{f}} + \boldsymbol{F}_{\mathrm{g}} = 0, \quad (6)$$

$$\rho_{\mathrm{s}} = \frac{\chi_{\mathrm{s}} - \chi_{\mathrm{m}}}{\mu_0 g} \left(B_z \frac{\partial B_z}{\partial z} + B_x \frac{\partial B_z}{\partial x} + B_y \frac{\partial B_z}{\partial y} \right) + \rho_{\mathrm{m}}. \quad (7)$$

3 Results and discussion

3.1 Simulation of a single-electromagnet levitation device

Experiments and simulations of electromagnet devices have shown that when current exists in the coil of the lower electromagnet and a pure iron core is used in the upper part, the magnetic field is highly favorable for the detection of magnetic Archimedes levitation (the magnetic field formed in this manner can generate a large product of magnetic induction intensity and magnetic induction intensity gradient) because when double electromagnets are used, the magnetic field is very small (the maximum magnetic induction intensity at the centerline is only 0.19 T). The magnetic field is 1.13 T and becomes six times that of double electromagnets when only one electromagnet is used. The shape of the electromagnet influences the distribution of the magnetic field considerably. The magnetic field of different structures are shown in Figs. 2(a)–2(c). The structure in Fig. 2(a) has a larger $|(\boldsymbol{B} \cdot \nabla)\boldsymbol{B}|$ compared with the other structures. The shape of the electromagnet in this experiment is conical, as shown in Fig. 2(a). The bottom radius of the cone is 65 mm, and its height is 40 mm. Compared with other shapes, conical electromagnets can produce greater magnetic induction. The magnetic field of a conical electromagnet is different from that of a permanent magnet. The magnetic induction intensity in Z direction is not linear. COMSOL software is used to simulate different situations. When the distance between poles increases, the magnetic induction intensity and gradient on the centerline decrease. At the levitation position, the vertical component of magnetic induction intensity is a quadratic curve.

An experiment is also performed for the case of 35 mm pole spacing. According to the theoretical calculation and simulation results, the magnetic induction intensity differs in the horizontal direction. The hovering position of the sample during the experiment is not in the middle. A cylindrical container with a radius of 5 mm is selected. The calculation results at the same offset are the same in any direction because the container is cylindrical, and the magnetic induction intensity is the same at the same distance in any direction. According to Eq. (4) and the simulation results, the value in X and Y directions in Eq. (4) is not zero, which causes the object to receive a horizontal force during levitation. Therefore, the movement of the sample in the horizontal direction needs to be limited by the container wall. By limiting the movement of the object in the horizontal direction, the force in the horizontal direction can be ignored. The values of $\left| B_z \frac{\partial B_z}{\partial z} + B_x \frac{\partial B_z}{\partial x} + B_y \frac{\partial B_z}{\partial y} \right|$ in the vertical direction are compared using COMSOL. The results show that $\left| B_z \frac{\partial B_z}{\partial z} \right|$ is much larger than $\left| B_x \frac{\partial B_z}{\partial x} + B_y \frac{\partial B_z}{\partial y} \right|$. Hence, only $B_z \frac{\partial B_z}{\partial z}$ is considered when the levitation height in the experiment is calculated. B_z is a two-order equation, and $\frac{\partial B_z}{\partial z}$ is a one-order equation. Thus, $B_z \frac{\partial B_z}{\partial z}$ can be written in the form of a cubic equation. The change in current does not affect the parameters in B_z and $\frac{\partial B_z}{\partial z}$ expressions and the parameters in $B_z \frac{\partial B_z}{\partial z}$ (a, b, c, and d in Eq. (9)). The magnetic induction intensity on the pole surface can be detected. Thus, the expression containing magnetic field intensity on the pole surface is used to represent the function of magnetic induction intensity on the central line. Hence, the calculation equations can be written as

$$\rho_{\mathrm{s}} = \frac{\chi_{\mathrm{s}} - \chi_{\mathrm{m}}}{\mu_0 g} \cdot B_z \frac{\partial B_z}{\partial z} + \rho_{\mathrm{m}} = f(z) + \rho_{\mathrm{m}}, \quad (8)$$

$$f(z) = \frac{\chi_{\mathrm{s}} - \chi_{\mathrm{m}}}{\mu_0 g} \cdot B_0^2 (az^3 + bz^2 + cz + d), \quad (9)$$

where B_0 is the magnetic induction intensity on the pole surface. B_0 changes linearly with the current.

3.2 Determination of the calculation equation

The experimental system can acquire a large measuring range by changing the magnetic induction intensity (current) and the concentration of the paramagnetic solution. The shape of the magnetic pole exerts a strong influence on the distribution of the magnetic field inside the electromagnet levitation device. By contrast, the upper and lower poles of a traditional permanent magnet magnetic levitation device are a plane. Using this kind of plane magnetic pole in the electromagnet experimental device will cause mutual cancellation of the magnetic field. The conical pole can exert a good converging effect on the magnetic field, and a large gradient of magnetic induction intensity and magnetic induction intensity is formed.

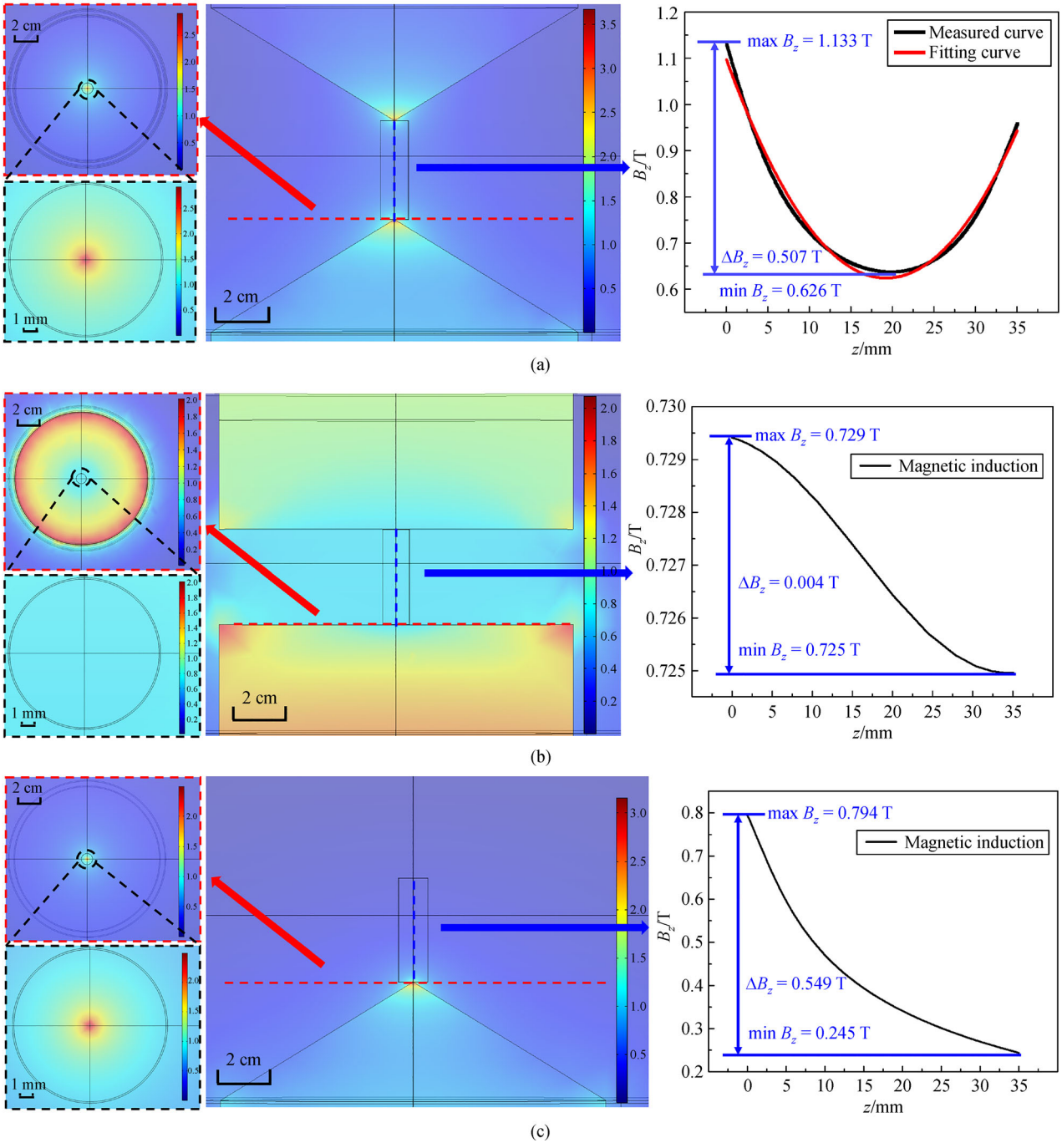

Fig. 2 Comparison of the effects of different structures. (a) A structure composed of a conical electromagnet in the lower part and a conical iron core in the upper part; (b) a structure composed of a cylindrical electromagnet at the bottom and a cylindrical iron core at the top; (c) a structure consisting of a single conical electromagnet.

The experimental system must be calibrated before detecting the substances (determine the values of a, b, c, and d in Eq. (9)). Spheres with densities of 1.35, 1.40, 1.45, and 1.50 g/cm^3 were used to verify the feasibility of the experiment. Standard-density balls were cleaned with alcohol. These standards, which were purchased from American Density Materials, Inc., USA, were certified according to the methods prescribed by American Society of Testing Materials by using measures and weights traceable to National Institute of Standards and Technology.

The distance between the lower pole of the electromagnet and the upper iron core was adjusted to 35 mm during the experiment. Then, different concentrations of $MnCl_2$ solution were prepared. An electronic balance with an accuracy of 0.01 g was used in the solution preparation

process to ensure high accuracy of solution concentration. In the calibration experiment, a 3 mol/L $MnCl_2$ aqueous solution was selected. The power supply was adjusted in the range of 0–15 A. When the current was 6 A, the magnetic induction intensity on the surface of the lower electromagnet pole was 0.8509 T. A cylindrical container with a bottom diameter of 10 mm was used. Vibration was applied during the experiment to eliminate the friction between the standard ball and the container wall. The levitation of the balls is shown in Fig. 3.

The levitation heights of the 1.35, 1.40, 1.45, and 1.50 g/cm^3 density balls were 15.65, 11.67, 9.93, and 8.27 mm, respectively. The density and magnetic susceptibility of the 3 mol/L $MnCl_2$ solution were 1.292 g/cm^3 and 5.49×10^{-4}, respectively. The magnetic susceptibility of the density ball was -5×10^{-6}. In accordance with these experimental data, the levitation height can be expressed as

$$f(z)=\frac{\chi_s-\chi_m}{\mu_0 g}\cdot B_0^2(1.01129\times10^{-5}z^3-2.89743\times10^{-4}z^2+1.82356\times10^{-3}z+5.35889\times10^{-3}). \quad (10)$$

The detection range of the experimental device under different concentrations of $MnCl_2$ aqueous solution was calculated with Eq. (10). The magnetic induction intensity of the surface of the pole was changed by adjusting the current. For example, when the concentration of the $MnCl_2$ aqueous solution was 3 mol/L, the measuring range of the experimental device was from 1.301 to 2.308 g/cm^3. At the same concentration of the $MnCl_2$ aqueous solution (3 mol/L), the measuring range of a magnetic levitation device built with a permanent magnet is from 1.15 to 1.50 g/cm^3 [1]. Comparison of the test results of the permanent magnet device and the electromagnet device under similar conditions showed that the experimental electromagnet device has a larger measuring range and can measure objects with higher density.

3.3 Verification experiment on different magnetic induction intensities

The advantage of the experimental electromagnet levitation device is its adjustability. The magnetic field can be controlled by changing the current. A standard ball with a density of 1.5 g/cm^3 was used to perform experiments under different surface magnetic induction intensities to

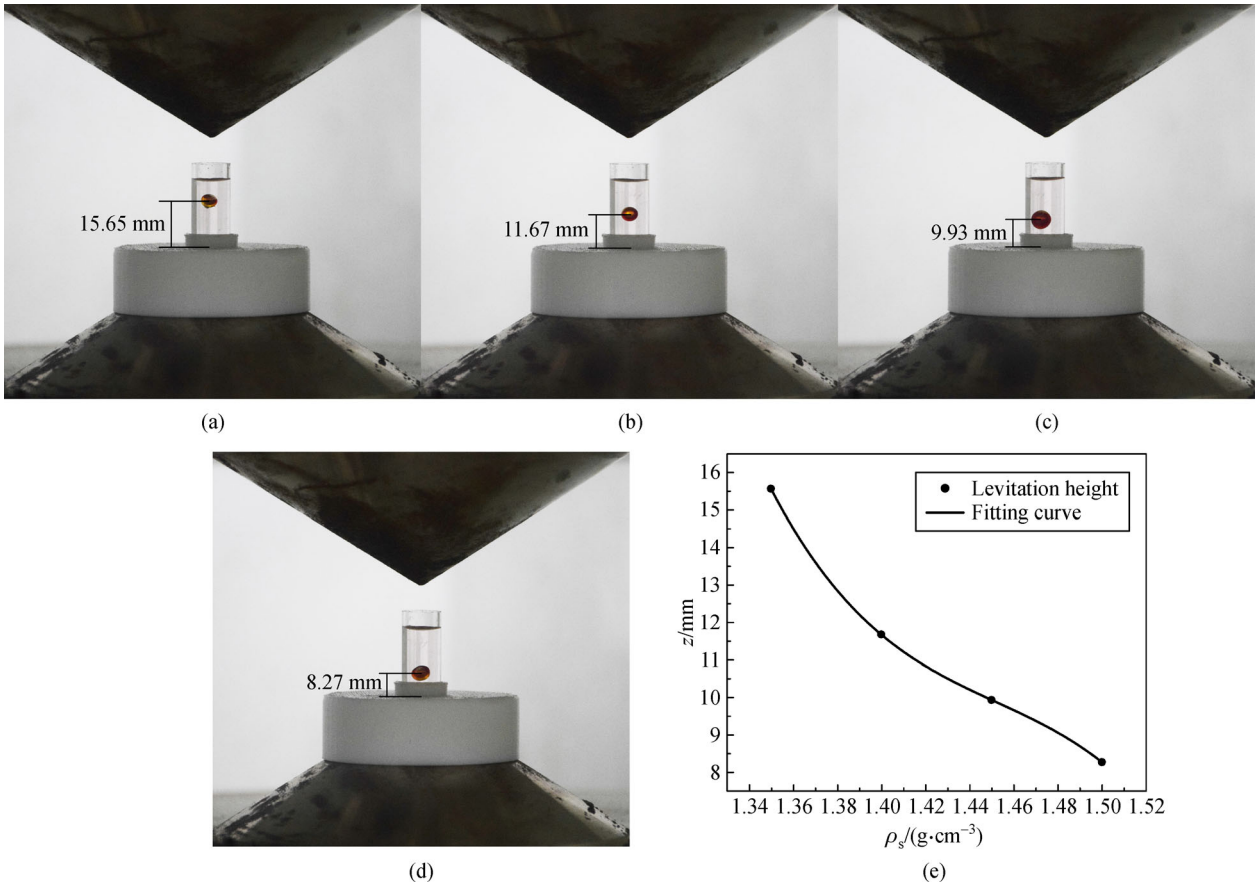

Fig. 3 Magnetic levitation detection of standard balls. Standard ball with (a) 1.35 g/cm^3 density, (b) 1.40 g/cm^3 density, (c) 1.45 g/cm^3 density, and (d) 1.50 g/cm^3 density; (e) statistical chart of levitated height data.

verify the accuracy of the formula. The standard ball was cleaned with alcohol, and a 3 mol/L $MnCl_2$ aqueous solution was prepared. A cylindrical container with a bottom diameter of 10 mm was used. The power supply was adjusted so that the surface magnetic induction intensity was 0.8398, 0.9933, 1.1196, 1.2148, 1.3546, 1.4429, 1.5679, 1.6129, 1.6568, and 1.6658 T. The levitation of the balls is shown in Fig. 4.

The experimental results in Figs. 4(a)–4(j) show that the same substance had different levitation heights under different surface magnetic induction intensities. Figure 4(k) indicates that the levitation heights calculated using Eq. (10) were in accordance with the measured levitation heights in the experiments. According to the experimental results, Eq. (10) is suitable for the case of different magnetic induction intensities on the surface of magnetic poles. The causes of errors were height measurement and friction from the vessel wall. The height measurement error can be reduced by using high-precision equipment, and the error of friction from the vessel wall can be reduced by means of vibration.

3.4 Density measurement for different substances

Several common substances with different densities were tested to verify the wide measuring range of the electromagnetic levitation device and the device's capability to achieve high precision. The levitation heights of the materials with different densities in the magnetic levitation detection device varied. This feature was used to measure the density of unknown-density materials. For the experiment, several common substances were prepared. For example, the densities of glass, carbon graphite plate, glass fiber, Teflon, and calcite were measured when the magnetic induction intensity was 1.6876 T and the concentration was 3.5 mol/L. The experimental results are shown in Fig. 5.

The levitation height of glass was 7.77 mm, and the calculated density was 2.3619 g/cm^3. The levitation height of the carbon graphite plate was 11.39 mm, and the calculated density was 1.8652 g/cm^3. The levitation height of the glass fiber was 8.98 mm, and the calculated density was 2.1986 g/cm^3. The levitation height of Teflon was 8.69 mm, and the calculated density was 2.2383 g/cm^3. The levitation height of calcite was 7.98 mm, and the calculated density was 2.3344 g/cm^3. The density results calculated using Eq. (10) agreed well with the actual values of different substances, as shown in Fig. 5(f). According to the experimental results, the device can accurately measure the density of different samples. However, the device is not very portable in its current form. In the future, the single-electromagnet device will be improved in terms of its design constraints for portability [24,25], for the integration of smartphone imaging [26,27], and for the integration of continuous stream of flow [28].

The experimental errors were mainly composed of the following: Medium density error ($\delta\rho_m$), magnetic susceptibility error ($\delta\chi_m$), height error (δz), and magnetic induction intensity error (δB_0). In Eqs. (8) and (9), χ_s is much smaller than χ_m. Therefore, the influence of χ_s on the final result can be ignored. The error of each parameter can be expressed by

$$\partial\rho_s(P) = \left|\frac{\partial\rho_s}{\partial P}\right|\delta P, \tag{11}$$

where P represents each variable that affects the calculated density of the sample. The error finally reflected in the detection density can be expressed by

$$\partial\rho_s = \sqrt{\left(\frac{\partial\rho_s}{\partial\rho_m}\delta\rho_m\right)^2 + \left(\frac{\partial\rho_s}{\partial\chi_m}\delta\chi_m\right)^2 + \left(\frac{\partial\rho_s}{\partial z}\delta z\right)^2 + \left(\frac{\partial\rho_s}{\partial B_0}\delta B_0\right)^2}. \tag{12}$$

The experimental group, in which ρ_s is 1.5 g/cm^3, B_0 is 1.665 T, χ_m is 5.49×10^{-4}, and ρ_m is 1.292 g/cm^3, was selected for error analysis. The analysis results are shown in Table 1. According to the results, the density measurement accuracy of the single-electromagnet levitation device is 0.001 g/cm^3.

3.5 Internal defect detection for aluminum alloy parts

The electromagnetic levitation device was used for internal defect detection in aluminum alloy, and the experimental method of controlling variables was adopted. Aluminum alloy cylinders with a section diameter of 4 mm and a length of 10 mm were manufactured manually from alloy 5052. This type of aluminum alloy is diamagnetic, so it is suitable for internal defect detection. A hole was drilled in the aluminum alloy parts to simulate internal defects. Numerical control machining was performed to process the parts. The defects were formed by drilling holes through the aluminum alloy, and a glue gun was used to block the two ends of the holes with a thin layer. This type of defect can change the density distribution inside the parts. The size and position of the internal defects varied in each aluminum alloy part, as shown in Fig. 6.

The defect size was unchanged in the first set of experiments, but the defect position of each sample differed. The effect of defect location on the tilt angle was then explored. In the second set of experiments, the defect location was unchanged, but the defect size of each sample differed. The effect of defect size on the tilt angle was also investigated. The parts were cleaned with alcohol and placed in the prepared $MnCl_2$ aqueous solution. The experimental conditions were as follows: the concentration of $MnCl_2$ was 4 mol/L, B_0 was 1.6876 T, and the distance was 45 mm. The levitation angle of a part was measured

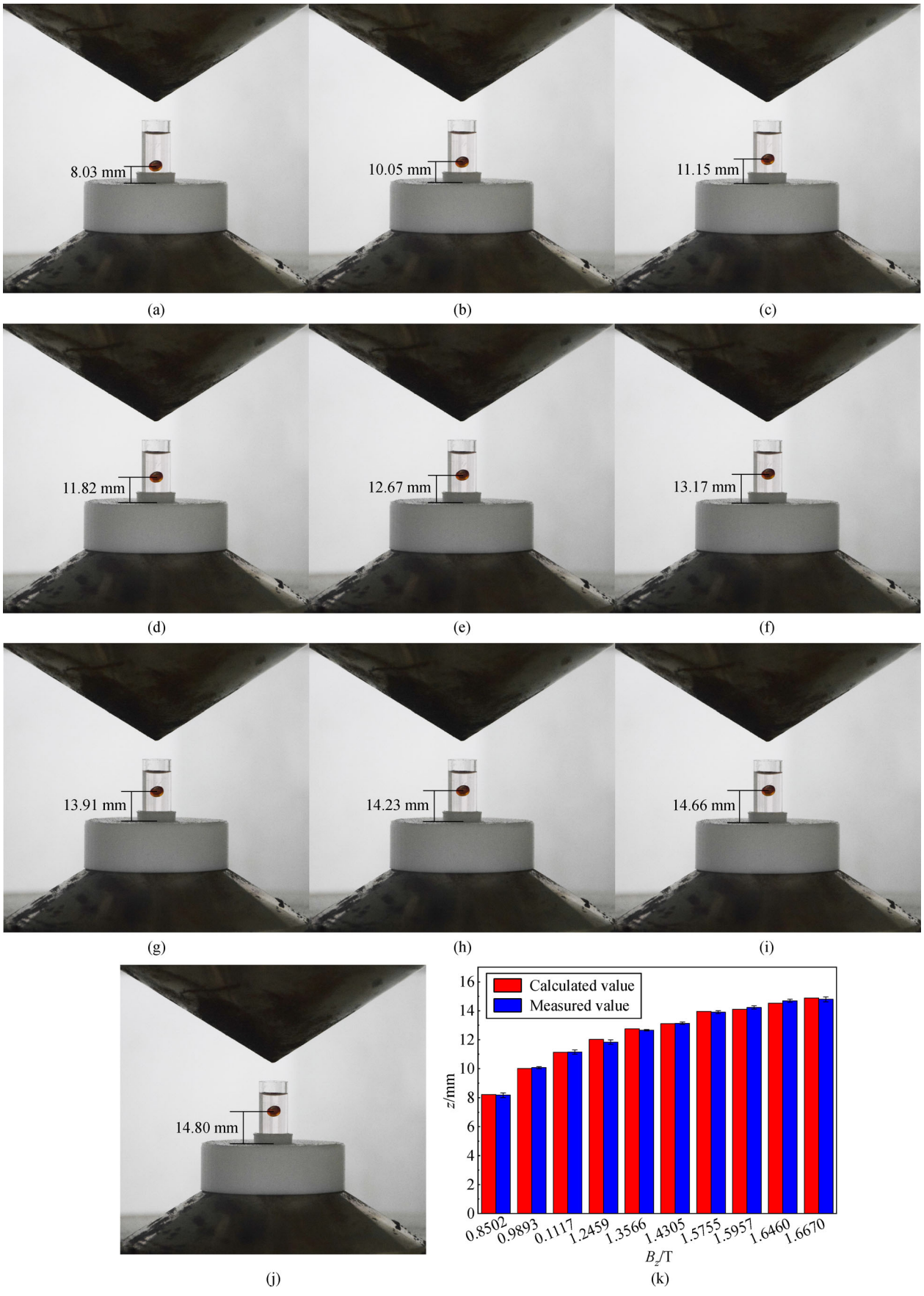

Fig. 4 Verification experiment on different magnetic induction intensities. Levitation height of (a) 8.03 mm, (b) 10.05 mm, (c) 11.15 mm, (d) 11.82 mm, (e) 12.67 mm, (f) 13.17 mm, (g) 13.91 mm, (h) 14.23 mm, (i) 14.66 mm, and (j) 14.80 mm; (k) statistical chart of theoretical and measured data.

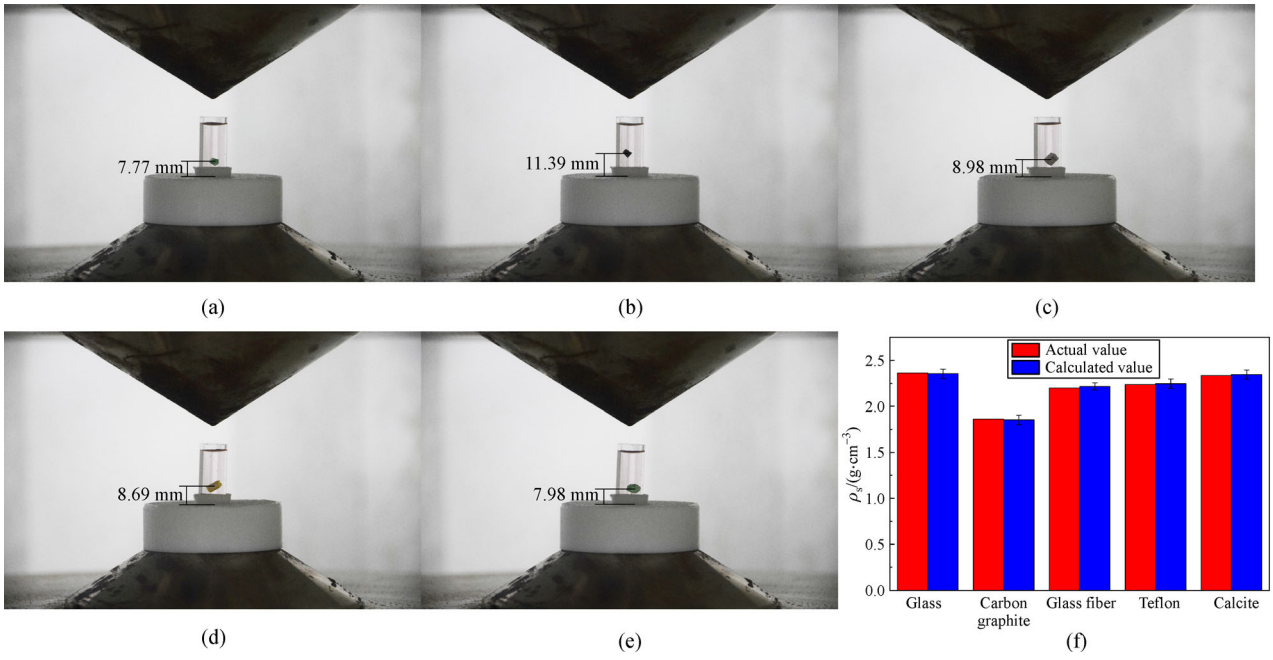

Fig. 5 Magnetic levitation testing of substances with different densities. Levitation of (a) glass, (b) carbon graphite plate, (c) glass fiber, (d) Teflon, and (e) calcite; (f) statistical chart of theoretical and measured data. χ_m is 6.465×10^{-4}, and ρ_m is 1.3404 g/cm^3. The test data in the figure are the average values of three measurements.

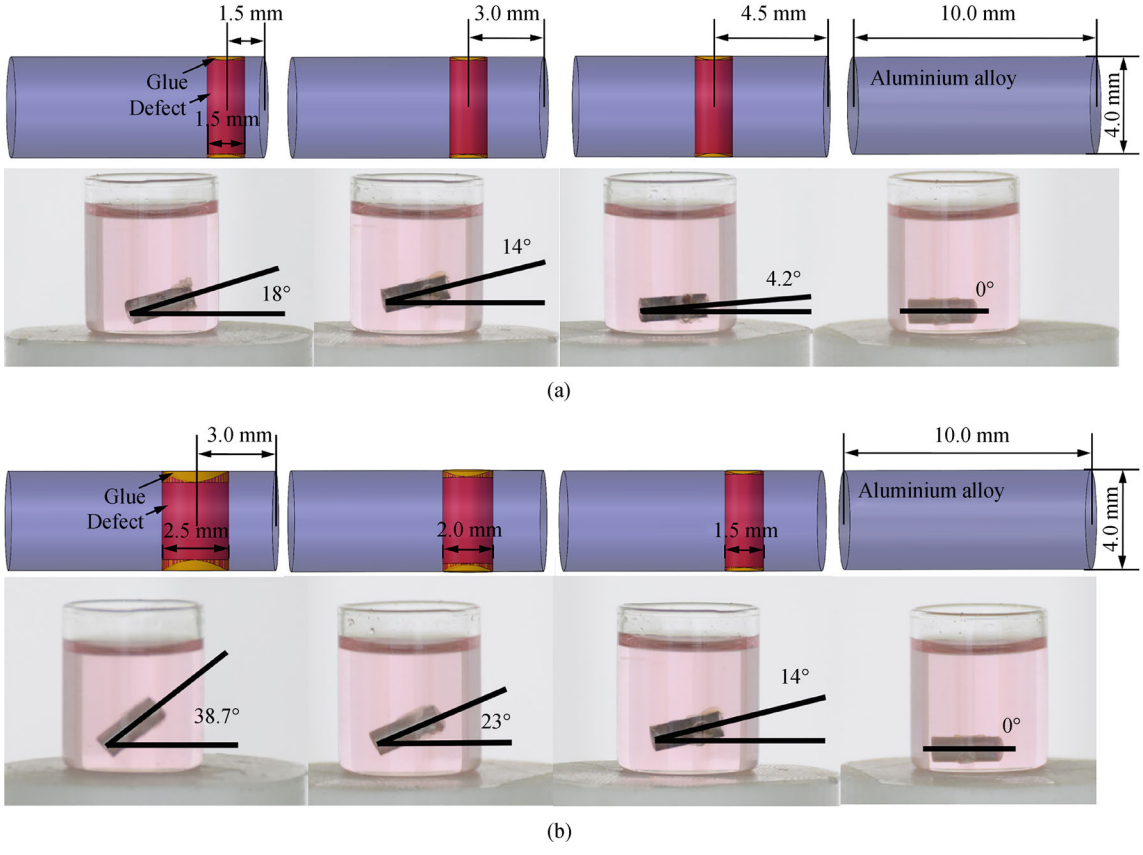

Fig. 6 Defect detection of aluminum alloy parts. (a) Defect locations are different; (b) defect sizes are different.

Table 1 Associated uncertainties of experimental parameters used in calculating ρ_s

P	Value of P	δP	$\delta\rho_s(P)/(g\cdot cm^{-3})$
B_0	1.665 T	±0.001 T	$\pm2\times10^{-9}$
χ_m	5.49×10^{-4}	$\pm1\times10^{-5}$	$\pm3\times10^{-8}$
ρ_m	1.292 g/cm^3	±0.001 g/cm^3	±0.001
μ_0	$4\pi\times10^{-7}$ N/A^2	n/a	n/a
g	9.8 m/s^2	n/a	n/a
z	14.80 mm	±0.01 mm	$\pm5\times10^{-9}$
ρ_s	1.5 g/cm^3		±0.001

after the part stabilized. The results are shown in Fig. 6. The experimental results indicated that the internal defects in the aluminum alloy parts caused an uneven distribution of internal density. The uneven density distribution led to a levitation angle of the aluminum alloy cylinder during magnetic levitation. Figure 6(a) shows that the farther the defect was from the center of the object, the larger the levitation angle was. The larger the defect was, the larger the levitation angle of the object was, as shown in Fig. 6(b). The objects without defects were levitated horizontally or vertically. Hence, the electromagnetic levitation device can be used to detect internal defects of aluminum alloy parts. For regular-shaped objects with defects inside, a certain deflection angle emerges in the process of magnetic levitation. A large levitation angle indicates that the internal defect is large or its position is far from the geometric center. The approaches used for identification and the specific calculation method have been discussed in previous studies. The tilt angle of samples with internal defects can be accurately calculated using the energy method [2,6].

4 Conclusions

This study analyzed the magnetic field distribution in a single-electromagnet levitation device for density measurement and defect detection. The following conclusions were obtained from the experiments:

1) Electromagnets can produce a large magnetic induction intensity gradient;

2) Unlike traditional magnetic levitation devices, the current device is suitable for samples with high density;

3) The single-electromagnet levitation device can realize density measurement and defect detection and has the advantages of convenient and rapid operation and wide applicability.

The device has good prospects for application in the detection of other high-density diamagnetic materials. The methods to improve the portability, intelligence, and continuous stream of flow will be discussed in subsequent research.

Acknowledgements The authors would like to acknowledge the financial support provided by the Key Research and Development Plan of Zhejiang Province (Grant No. 2020C01113), the National Natural Science Foundation of China (Grant Nos. 51821093 and 51875519), and Zhejiang Provincial Natural Science Foundation of China (Grant No. LZ18E050002).

Conflict of interest The authors declare that they have no conflict of interest.

References

1. Mirica K A, Shevkoplyas S S, Phillips S T, et al. Measuring densities of solids and liquids using magnetic levitation: Fundamentals. Journal of the American Chemical Society, 2009, 131(29): 10049–10058
2. Xia N, Zhao P, Xie J, et al. Non-destructive measurement of three-dimensional polymeric parts by magneto-Archimedes levitation. Polymer Testing, 2018, 66: 32–40
3. Yenilmez B, Knowlton S, Yu C H, et al. Label-free sickle cell disease diagnosis using a low-cost, handheld platform. Advanced Materials Technologies, 2016, 1(5): 1600100
4. Simon M D, Geim A K. Diamagnetic levitation: Flying frogs and floating magnets (invited). Journal of Applied Physics, 2000, 87(9): 6200–6204
5. Waldron R D. Diamagnetic levitation using pyrolytic graphite. Review of Scientific Instruments, 1966, 37(1): 29–35
6. Xia N, Zhao P, Xie J, et al. Defect diagnosis for polymeric samples via magnetic levitation. NDT & E International, 2018, 100: 175–182
7. Xie J, Zhao P, Zhang C, et al. A feasible, portable and convenient density measurement method for minerals via magnetic levitation. Measurement, 2019, 136: 564–572
8. Zhang C, Zhao P, Tang D, et al. Axial magnetic levitation: A high-sensitive and maneuverable density-based analysis device. Sensors and Actuators. B, Chemical, 2020, 304: 127362
9. Zhang C, Zhao P, Gu F, et al. Axial-circular magnetic levitation: A three-dimensional density measurement and manipulation approach. Analytical Chemistry, 2020, 92(10): 6925–6931
10. Zhang C, Zhao P, Wen W, et al. Density measurement via magnetic levitation: Linear relationship investigation. Polymer Testing, 2018, 70: 520–525
11. Xie J, Zhao P, Jing Z, et al. Research on the sensitivity of magnetic levitation (MagLev) devices. Journal of Magnetism and Magnetic Materials, 2018, 468: 100–104
12. Xie J, Zhang C, Gu F, et al. An accurate and versatile density measurement device: Magnetic levitation. Sensors and Actuators. B,

Chemical, 2019, 295: 204–214
13. Lockett M R, Mirica K A, Mace C R, et al. Analyzing forensic evidence based on density with magnetic levitation. Journal of Forensic Sciences, 2013, 58(1): 40–45
14. Atkinson M B J, Bwambok D K, Chen J, et al. Using magnetic levitation to separate mixtures of crystal poly-morphs. Angewandte Chemie International Edition, 2013, 125(39): 10398–10401
15. Zhang X, Gu F, Xie J, et al. Magnetic projection: A novel separation method and its first application on separating mixed plastics. Waste Management (New York, N.Y.), 2019, 87: 805–813
16. Subramaniam A B, Yang D, Yu H D, et al. Noncontact orientation of objects in three-dimensional space using magnetic levitation. Proceedings of the National Academy of Sciences of the United States of America, 2014, 111(36): 12980–12985
17. Zhang C, Zhao P, Gu F, et al. Single-ring magnetic levitation configuration for object manipulation and density-based measurement. Analytical Chemistry, 2018, 90(15): 9226–9233
18. Hennek J W, Nemiroski A, Subramaniam A B, et al. Using magnetic levitation for non-destructive quality control of plastic parts. Advanced Materials, 2015, 27(9): 1587–1592
19. Xia N, Zhao P, Xie J, et al. Density measurement for polymers by magneto-Archimedes levitation: Simulation and experiments. Polymer Testing, 2017, 63: 455–461
20. Xie J, Zhao P, Zhang C, et al. Measuring densities of polymers by magneto-Archimedes levitation. Polymer Testing, 2016, 56: 308–313
21. Knowlton S, Yu C H, Jain N, et al. Smart-phone based magnetic levitation for measuring densities. PLoS One, 2015, 10(8): e0134400
22. Zhao P, Xie J, Gu F, et al. Separation of mixed waste plastics via magnetic levitation. Waste Management, 2018, 76: 46–54
23. Zhang C, Zhao P, Xie J, et al. Enlarging density measurement range for polymers by horizontal magneto-Archimedes levitation. Polymer Testing, 2018, 67: 177–182
24. Yenilmez B, Knowlton S, Tasoglu S. Self-contained handheld magnetic platform for point of care cytometry in biological samples. Advanced Materials Technologies, 2016, 1(9): 1600144
25. Amin R, Knowlton S, Dupont J, et al. 3D-printed smartphone-based device for label-free cell separation. Journal of 3D Printing in Medicine, 2017, 1(3): 155–164
26. Knowlton S, Joshi A, Syrrist P, et al. 3D-printed smartphone-based point of care tool for fluorescence- and magnetophoresis-based cytometry. Lab on a Chip, 2017, 17(16): 2839–2851
27. Knowlton S M, Sencan I, Aytar Y, et al. Sickle cell detection using a smartphone. Scientific Reports, 2015, 5(1): 15022
28. Amin R, Knowlton S, Yenilmez B, et al. Smart-phone attachable, flow-assisted magnetic focusing device. RSC Advances, 2016, 6(96): 93922–93931